CANADIAN JOURNAL OF EXPLORATION GEOPHYSICS
VOL. 34, NOS. 1 & 2 (DECEMBER 1998), P. 30-39

# HRAM FAULT INTERPRETATION USING MAGPROBE™ DEPTH ESTIMATES AND NON-TRADITIONAL FILTERING

SERGUEI A. GOUSSEV[1], ROBERT A. CHARTERS[1], HASSAN H. HASSAN[1], JOHN W. PEIRCE[1] AND JAMES A. GENEREUX[2]

## ABSTRACT

We discuss in this paper a technique for interpreting high resolution aeromagnetic (HRAM) data to identify and correlate intra-sedimentary and upper basement vertical and near vertical magnetized faults. In this technique we integrate the results of two independent approaches: 1) interpretation of Magprobe™ automatic depth estimations; and 2) interpretation of filtered magnetic maps. Cascaded Goussev filtering, a new and successful technique, is discussed. This two-pronged interpretation technique generally assumes that magnetized faults can be approximated by thin dike causative bodies. In practice, magnetized faults appear to be a narrow vertical distribution of heterogeneous sources. An example from the Simonette region of Alberta, Canada, shows that the sealing fault separating two hydrocarbon pools defined by 3D seismic data can be reliably identified and correlated beyond the limits of the seismic survey area using our integrated processing and interpretation technique. The results illustrate conclusively that carefully processed and interpreted HRAM data can contribute significantly to regional petroleum exploration and to development geophysics at the prospect level.

## INTRODUCTION

Vertical and near vertical intra-sedimentary faults originate from changes in the regional stress fields both within the metamorphic basement and the sedimentary section. Faults and fractures can provide channels for basement fluids to move across laterally continuous barriers to vertical fluid migration (Davies, 1997). These upwardly mobile basement fluids can enter into chemical reactions with host sedimentary rocks that may result in conditions favorable to the precipitation of magnetic minerals in the vicinity of the fault or fracture system (Peirce et al., 1998b). Relatively high concentrations of magnetic minerals along intra-sedimentary faults can produce low magnitude, high frequency anomalies which are detectable by HRAM surveys (Jain, 1986; Ebner et al., 1995; Peirce et al., 1998a).

## INTERPRETATION APPROACH

In the spatial frequency domain, intra-sedimentary and upper basement faults tend to have significant energy in the mid to high frequency bands of the observed total magnetic field (i.e., wavelengths from 200 m to 4000 m). We often observe that the intensity of magnetic signals generated from intra-sedimentary sources is one to several orders of magnitude less than signals generated from within the metamorphic basement. The detection of these weak intra-sedimentary signals is often complicated by the superposition of the stronger, low frequency basement and regional events, interference with adjacent anomalies from the same depth range, and high levels of background noise. To separate and effectively enhance intra-sedimentary anomalies, the processing of HRAM data should address: 1) removal of low frequency high amplitude regional signals; 2) attenuation of background noise; 3) enhancement of higher frequency, low amplitude residuals; and 4) increased lateral resolution to resolve interfering anomalies.

## MAGPROBE™ DEPTH ESTIMATES

Magprobe™ is an LCT Inc. software package designed to isolate specific anomalies in magnetic field profiles and to apply a number of different interpretive analyses to obtain a depth to top and basic geometry for the causative magnetic body. Magprobe™ can also be run in batch mode, whereby the depth analyses are performed in gates of various lengths that move systematically along the magnetic profile (Jain, 1976). The two depth analyses best suited to this automatic mode are Werner deconvolution (Werner, 1953; Ku and Sharp, 1983) and Euler (2D) modeling (Thompson, 1983). Given proper specification of parameters, both techniques are sensitive to basement and intra-sedimentary sources. The Werner deconvolution method uses the total field to calculate depth solutions for dipping thin dike source geometries and the horizontal derivative of the total field to calculate depth solutions for dipping magnetic contact surfaces. The Euler technique uses the total field and specifies the source geometry through a structural index (e.g., a structural index of 0-1 represents sources that are strongly linear and two dimensional in nature, while an index of 2-3 represents sources that are massive and three dimensional). We typically

[1]GEDCO, Suite 1200, 815-8th Ave SW, Calgary, Alberta, Canada T2P 3P2
[2]Spectra Exploration Geoscience, Suite 2620, 520-5th Ave SW, Calgary, Alberta, Canada T2P 3R7

use a structural index in the range of 1.0-1.7 for the first pass over the data set, so the calculation will be sensitive to both faults and deeper 3D structures. Note that once a fault or magnetic body has been identified with these Euler parameters, the structural index is refined to better image the anomaly-related source depth estimates. Each depth calculation, for either the Werner or Euler technique, is run for a wide variety of gate widths, usually 15-20 different gates depending on the frequency content of the anomalies being interpreted. The gate width determines the focus on deeper or shallower solutions. Deep sources create long wavelength anomalies and therefore require longer gates for their identification, while shallower sources are detected with shorter gates. A rule of thumb is that the gate length must be at least one-half the dominant wavelength of the anomaly. The final depth estimate is actually the RMS location of a cluster of raw solutions (e.g., 6, solutions within a 250 m x 250 m box) for a given gate and therefore represents a statistical average of approximations of the actual location and depth of the causative magnetic source.

The Magprobe™ depth estimates are easily contaminated by noise and superposition of anomalies which can result in spurious raw picks, which in turn perturb the position of the clustered solution in a given section. In our HRAM interpretation technique, Magprobe™ is run on all the observed HRAM profiles systematically. Depth profiles from the automatic depth estimates are plotted and interpreted. Vertical or near vertical alignments of depth estimates are interpreted to be associated with faults. We should note here that not all vertical alignments of depth solutions are necessarily attributable to faults. It is well known that Werner depth estimates over a thin dike can decrease with a decrease in the gate length (Jain, 1976). However, the degree of vertical dispersion in depth solutions that we interpret as faults is often significantly greater than the dispersion due to decreasing gate length. This is particularly evident in the Magprobe™ interpretations of 2D models of the vertical dikes shown in Figure 1. We have observed that such major alignments are common within the upper basement and intra-sedimentary section and interpret them to be the response to non-uniform magnetization and dip along the fault or associated fracture system. We believe that only those faults and fractures with a history of fluid flow are likely to be magnetized (Peirce et al., 1998b). Within the basement, these alignments indicate either similar faults as mentioned above or contacts between blocks of contrasting susceptibility. Other estimates that do not correlate within the profile are treated as noise. In order for a given alignment to be confirmed as a fault expression, it must be correlatable across neighboring profiles of the HRAM survey. Sometimes, making this correlation between Magprobe™ sections is difficult. This is where the second step of our technique, the interpretation of filtered magnetic field maps, is applied. Close comparison of the filtered maps with the Magprobe™ interpretation allows a more confident correlation of fault anomalies from one profile to another, and thereby facilitates the construction of the intra-sedimentary and basement structure grain maps. These are maps that show the location of and depth to major faults, contacts and plutonic bodies that are affecting the geologic structure being investigated. Although using filtered field maps to help correlate profile interpretations is standard geophysical practice, it is the type of map used herein that is unique.

## Cascaded Goussev Filtering

Magprobe™ generally produces good resolution of the depth to magnetic sources, but the Magprobe™ data is often difficult to correlate laterally across profiles, particularly for weak anomalies. Filtered field maps can provide better lateral correlation of anomalies, but suffer from spectral leakage of the signal from one depth interval to another. In other words, it is difficult to separate clearly the signal from deep sources from the signal from shallow sources. Cascaded Goussev Filtering (CGF) addresses this as well as other issues concerning noise and lateral resolution.

We apply CGF in order to: a) attenuate dominating regional components which mask the residual components of geologic interest; b) suppress irregular and spurious noise; and c) enhance the lateral resolution of anomalies identified in the residual field.

CGF consists of three steps. First an attempt is made to restrict the signal to a particular depth interval (intra-sedimentary sources or deeper basement sources). There are various published techniques which attempt to achieve this separation. The most common techniques are based on spectral resolution (e.g., Spector and Grant, 1970). Unfortunately significant spectral leakage between anomalies commonly hampers the success of these approaches. Spectral leakage is one of the inherent properties of potential fields that reflects the fundamental ambiguity with respect to interpreting source depths and geometries. It is the spectral overlap of predominantly long wavelength deep source anomalies with predominantly short wavelength shallow source anomalies. We prefer to use separation filtering based on upward continuation of the observed signal as described by Jacobsen (1987). Leakage in Jacobsen's separation filtering tends to occur at longer wavelengths within the chosen bandwidth since the operators are quasi-exponential. This leakage at the low end is addressed by the second step of CGF.

The second step of CGF consists of taking the scalar difference between the total gradient of the magnetic field (TG, otherwise known as the analytic signal) and the horizontal gradient of the magnetic field (HG). The magnetic field in this case is the separated field resulting from the first step. This scalar difference in gradients is essentially a filtered approximation of the vertical gradient (VG), where long wavelengths have been suppressed and short wavelengths have been enhanced. Indeed, at extrema in the magnetic field signal, this difference in gradients is precisely equal to the VG.

The total magnetic field can be expressed as a sum of three components: a long wavelength regional component, a

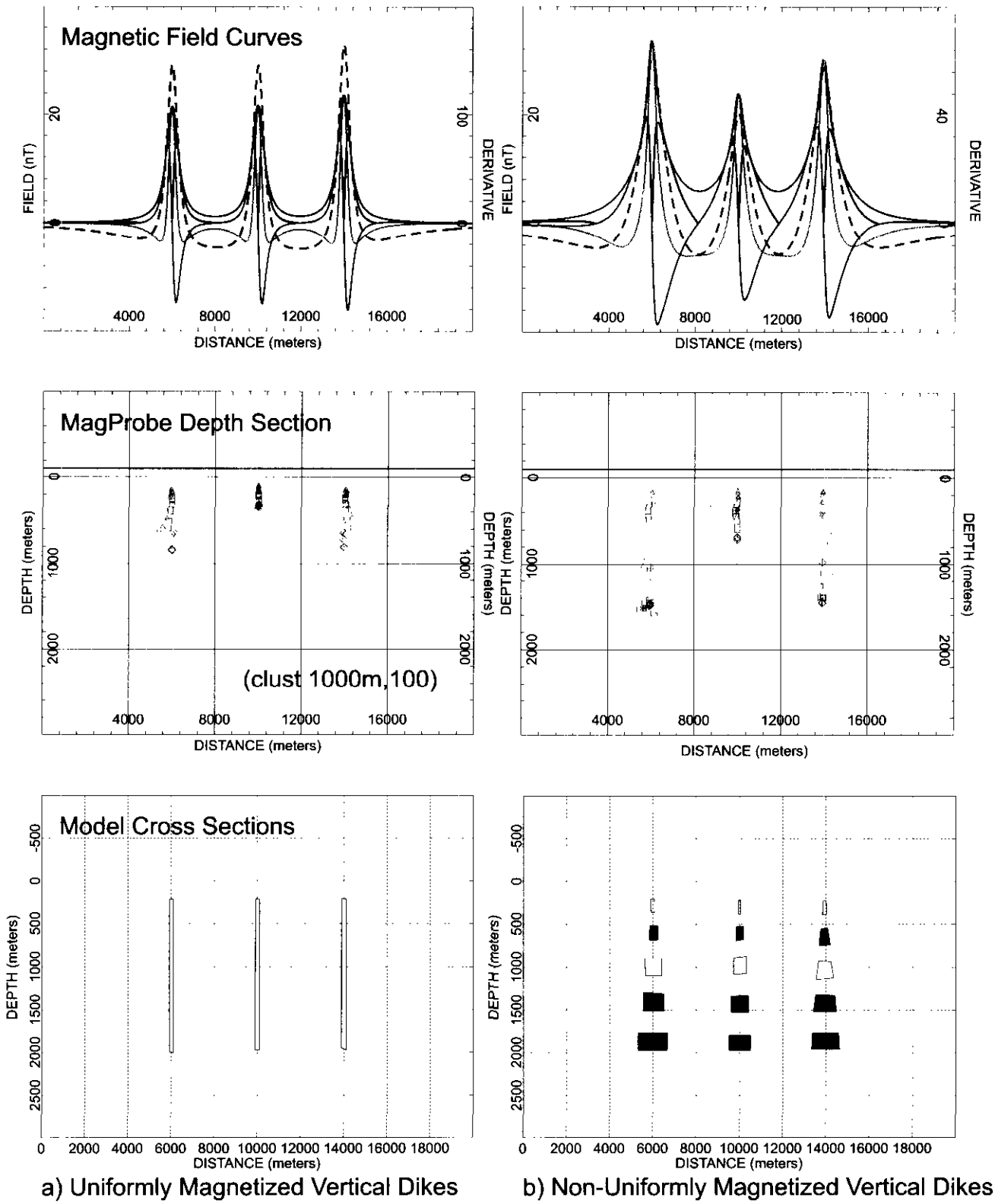


**Fig. 1.** Two-dimensional models of uniformly magnetized dikes and non-uniformly magnetized dikes. Shown in the top panels are the synthetic total magnetic field curves and their gradients. The center panels show the Magprobe™ depth interpretations of the calculated fields. Shown in red are the Werner depth estimates and in green, the Euler depth estimates. The raw depth solutions have been clustered with a minimum of 100 raw picks per group and a minimum separation of 1000 m between groups. The bottom panels show the cross sections of the 2D models. The pattern of increasing magnetization and increasing width with depth as shown in the lower right panel is the only model that we have found for which the magnetic response resembles the response we observe in real data.

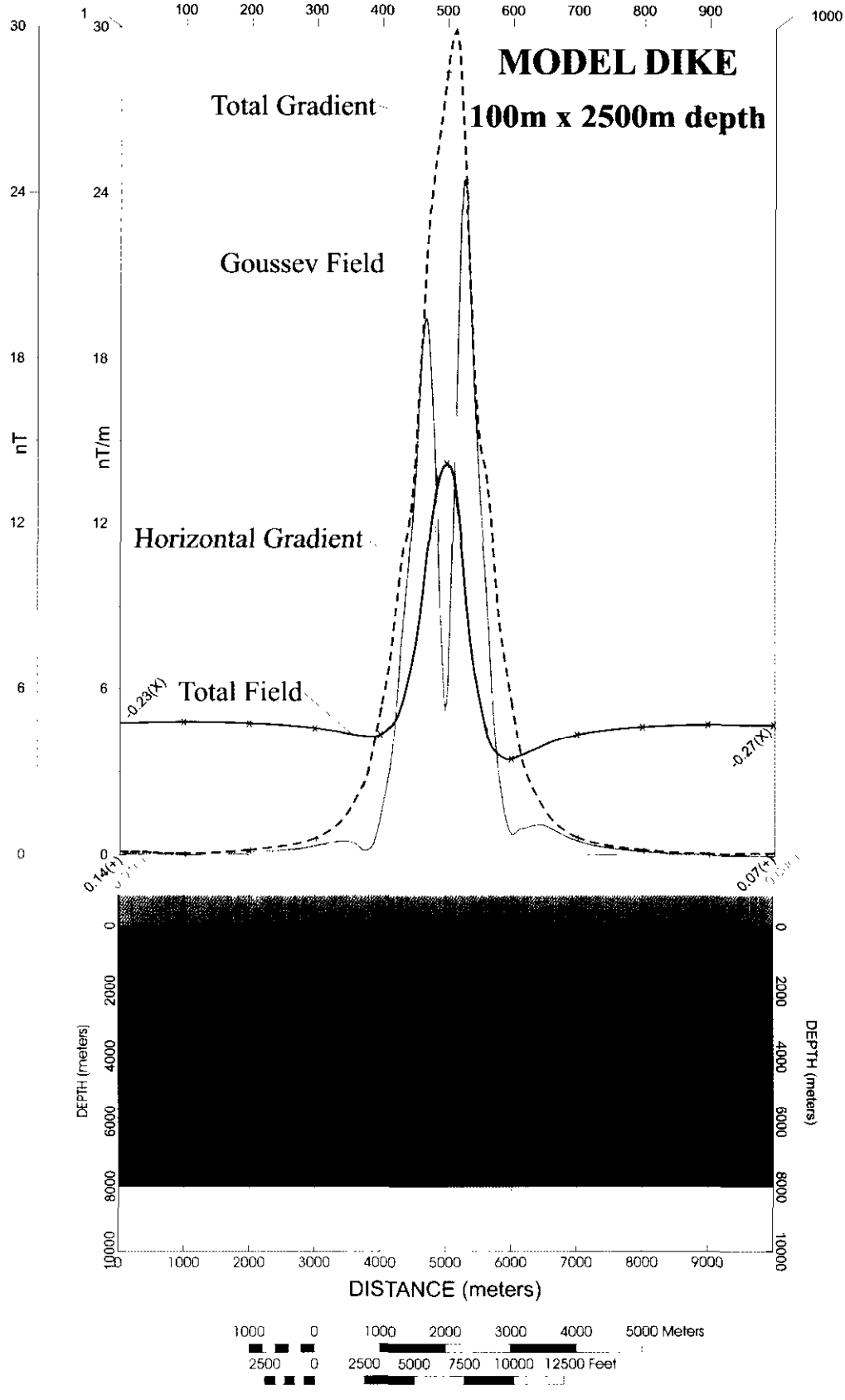


**Fig. 2.** Two-dimensional model of the magnetic field over a thin vertical dike. The direction of the profile is perpendicular to the strike of the dike. The magnetization contrast of the dike is 4000 micro-cgs units, and the top is at 2500 m depth.

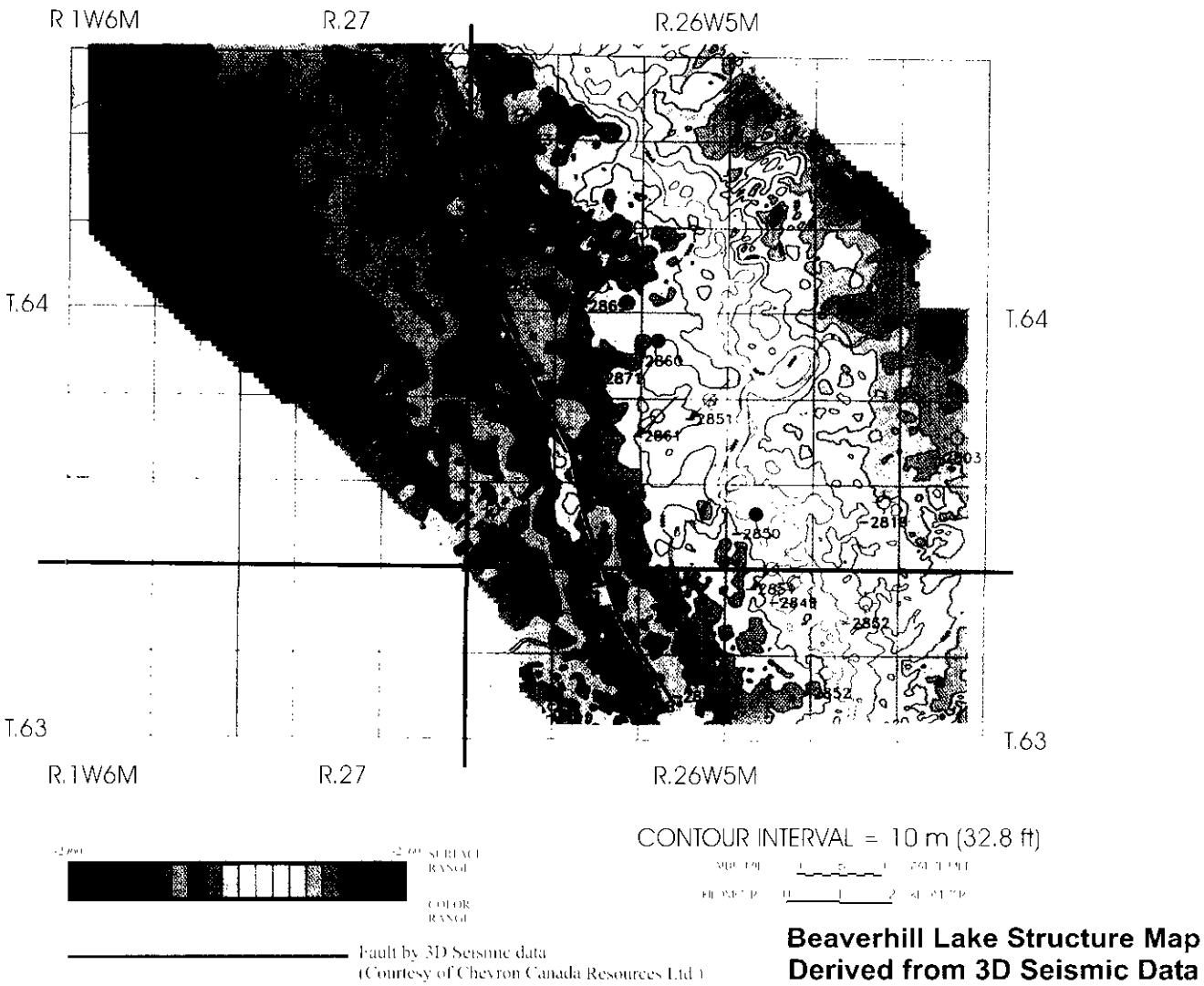


**Fig. 3.** Structure map of the Beaverhill Lake hydrocarbon pool in the Simonette region of Alberta, Canada (Chevron Canada Resources Ltd.). The interpretation was derived from a 3D seismic survey. The sealing fault between the "A" and "B" pools is shown in yellow

middle and short wavelength residual component; and additive short wavelength noise, i.e.,

$$TF = Reg(TF) + Res(TF) + Ns(TF) \quad (1)$$

Likewise, the total and horizontal gradient fields can be expressed as

$$TG = Reg(TG) + Res(TG) + Ns(TG),$$
$$HG = Reg(HG) + Res(HG) + Ns(HG). \quad (2)$$

Hence,

$$TG - HG = \{Reg(TF) - Reg(HG)\} + \{Res(TG) - Res(HG)\} + \{Ns(TG) - Ns(HG)\}. \quad (3)$$

Equation (3) helps us to understand conceptually the effect of this difference field. Energy at long wavelengths contained in the regional fields common to TG and HG is suppressed by the difference. Likewise, white noise passing through the gradient operators is also suppressed by the difference operator, whereas it would be amplified by a simple vertical gradient operator. This leaves the principal energy in Equation (3) at mid to high frequencies with respect to the residual anomaly bandwidth. We can see this effect empirically in the 2D model of a vertical dike in Figure 2, where the total magnetic field and its derivatives are shown for a profile over a 100 m wide dike perpendicular to the strike direction. The fields are reduced to the pole. As one can clearly see, the TG has its maximum value centered over the dike, while the HG has a minimum at the same point. So the scalar difference (TG – HG), as defined by the Goussev filter curve, defines a narrower local anomaly of mid to high frequency content with adjacent side lobes.

We can see how the second step of CGF successfully attenuates long regional wavelengths associated with source field leakage, while enhancing the lateral resolution of the magnetic anomaly. As will be seen in the following example, the CGF can dramatically resolve overlapping anomalies of different bandwidths.

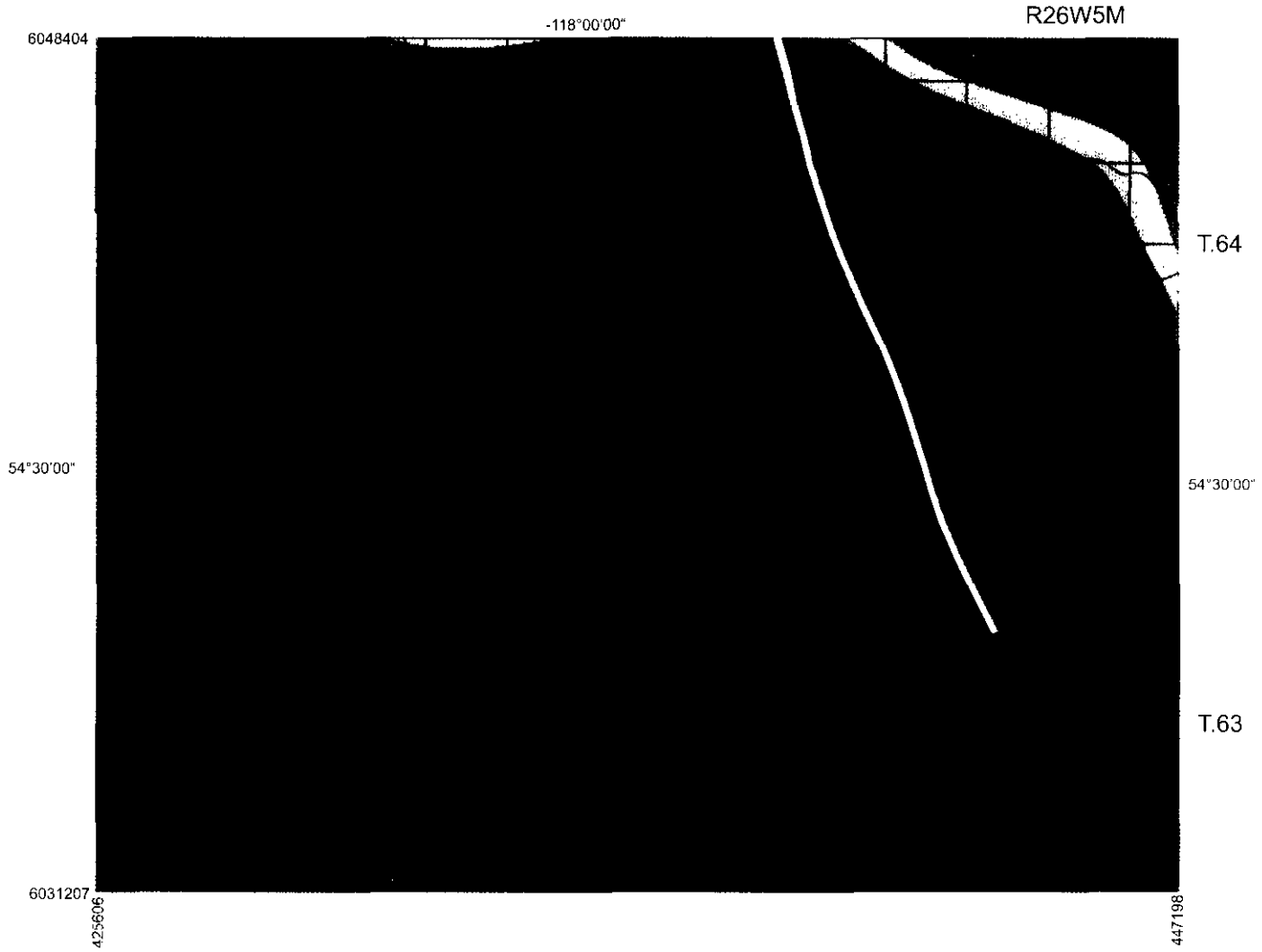


**Fig. 4.** Total Magnetic Field data from the Simonette HRAM survey over the Beaverhill Lake pool. Note the broad trough parallel to the seismically imaged sealing fault (yellow line). This long wavelength feature is an expression of basement structure rather than the intra-sedimentary sealing fault.

The third and last step of Cascaded Goussev Filtering is the application of traditional filtering procedures (e.g., bandpass filters or successive vertical derivatives) that lead to a further improvement of lateral resolution. Note that after suppression of spurious noise by the difference calculation, subsequent application of the vertical derivative operator is even more effective at enhancing linear trends and boundaries.

In our experience the two-pronged interpretation technique described above has proven to be far more effective (in terms of signal to noise ratios) for the interpretation of intra-sedimentary anomalies than conventional spectral and gradient analyses and filtering of HRAM data.

## The Simonette, Alberta, Example

This example is taken from the Simonette area of west central Alberta, Canada. Here we examine the hydrocarbon bearing Beaverhill Lake (Devonian) Structure defined by 3D seismic data and, in particular, the sealing fault that separates the "A" and "B" pools of the field (Fig. 3). Figure 4 shows a portion of the Swan Hills HRAM survey flown over the field. Note that a broad trough in the total magnetic field generally follows the interpreted seismic fault. This will be shown to be related to basement sources. Figure 5 shows a traditional high frequency bandpass filter of this data (0.8-2.4 km), which has been tuned to intra-sedimentary depths. The anomaly associated with the sealing fault is still hidden in the trough. Figure 6 shows the application of Cascaded Goussev Filtering to the total field data. The CGF parameters were also tuned to the intra-sedimentary interval. Clearly, CGF dramatically separates and resolves the high frequency magnetic anomaly associated with the sealing fault from the superposing long wavelength trough. The CGF fault anomaly is offset to the west of the seismically imaged fault for several reasons as shown in Figure 7.

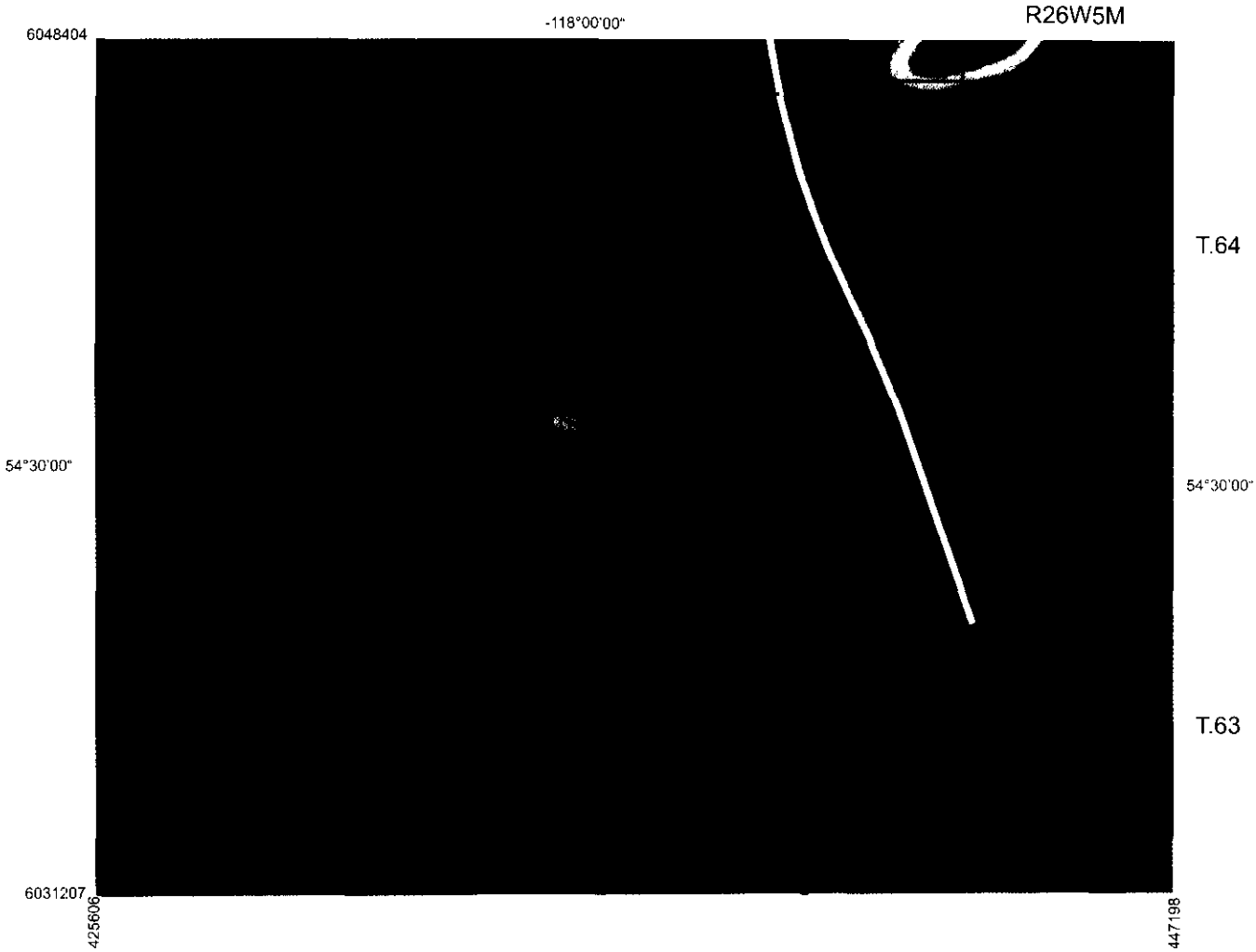


**Fig. 5.** Traditional high frequency bandpass filter (0.8-2.4 km) of the total field data. This bandpass should be sensitive to sources in the intra-sedimentary interval; however, the expression of the sealing fault is still hidden in middle wavelengths from the basement related trough. The yellow line is the position of the seismically imaged fault.

Figure 7 shows our detailed interpretation of an east-west profile of HRAM data crossing almost orthogonally to the sealing fault. The upper portion of the figure shows the total magnetic field profile along with the traditional filtered curves and two examples of CGF processed curves. The lower part of the figure shows an interpretation of the Magprobe™ depth section along the profile. Points in red are depth estimates derived from Werner Deconvolution solutions, while points in green are depth estimates derived from 2D Euler solutions using a structural index of 1.2. Significant vertical and near vertical alignments of depth estimates are present in the immediate vicinity of the fault and are interpreted to represent at least two splays of the sealing fault system. This interpretation indicates that the sealing fault(s) dips to the east and is listrically rooted to the main basement structure, which appears to be a major contact with vertical offset. This basement structure controls the long wavelength component of the total magnetic field (expressed as a broad trough), which totally masks the small magnitude, short wavelength anomaly due to the sealing fault. However, CGF processing (curves 4 and 5), being tuned to the intra-sedimentary interval, successfully extracts the image of the sealing fault from the interfering and superposing basement events.

The CGF fault anomaly is offset from the seismic fault trace to the west for two principal reasons: 1) the sealing faults are dipping to the east. This positions magnetic sources above and to the west of the location of the seismic fault at the Beaverhill Lake level, and 2) there appear to be at least two splays in the sealing fault and the listric nature of the deeper splay again may carry more magnetic sources west of the seismic fault location.

Figure 7 also demonstrates the effectiveness of combining the interpretation of Magprobe™ depth analysis with CGF mapping analysis in determining the nature and location of the sealing fault.


**Fig. 6.** Cascaded Goussev Filter of the total field data. The CGF parameters have been tuned to intra-sedimentary depths. Notice how the magnetic expression of the sealing fault can be seen clearly, although it is offset to the west of the seismically defined fault (yellow line). The CGF process has successfully extracted the weak sealing fault response from the superposed strong basement response.

## Conclusions

Our two-pronged approach to HRAM interpretation, which combines the independent analysis of Magprobe™ depth sections with the analysis of filtered maps of gridded field data, provides a most effective and objective means to identify and correlate intra-sedimentary and upper basement magnetized faults.

The Simonette example shows how intra-sedimentary magnetized faults can be identified and correlated in the context of a much larger basement signal. Cascaded Goussev Filtering can provide significantly better enhancement of low magnitude residual high frequency anomalies of the total magnetic field, as well as higher lateral resolution of interfering anomalies as compared to traditional cascaded filtering procedures.

Our experience in comparing numerous interpretations of HRAM surveys to seismic control is that only a modest percentage (perhaps 25 per cent) of seismically observed faults are detectable magnetically. However in some cases we believe that we can detect magnetized fractures that are not detectable seismically because they have little or no throw. Furthermore, we hypothesize that the faults and fractures, which are detectable magnetically, are those which have had a fluid flow history; this may be very important information to assist in understanding the development of fracture porosity (e.g., hydrothermal dolomitization), migration and fault seal problems (Peirce et al., 1998b).

The pattern of the magnetized faults and fractures detected from interpretation of HRAM surveys does provide an indication of the structural grain of an area, both in terms of fault orientation and fault density. This can be very useful for seismic planning, in order to optimize the placement of new seismic lines, and in seismic interpretation of widely spaced lines to guide fault correlation.

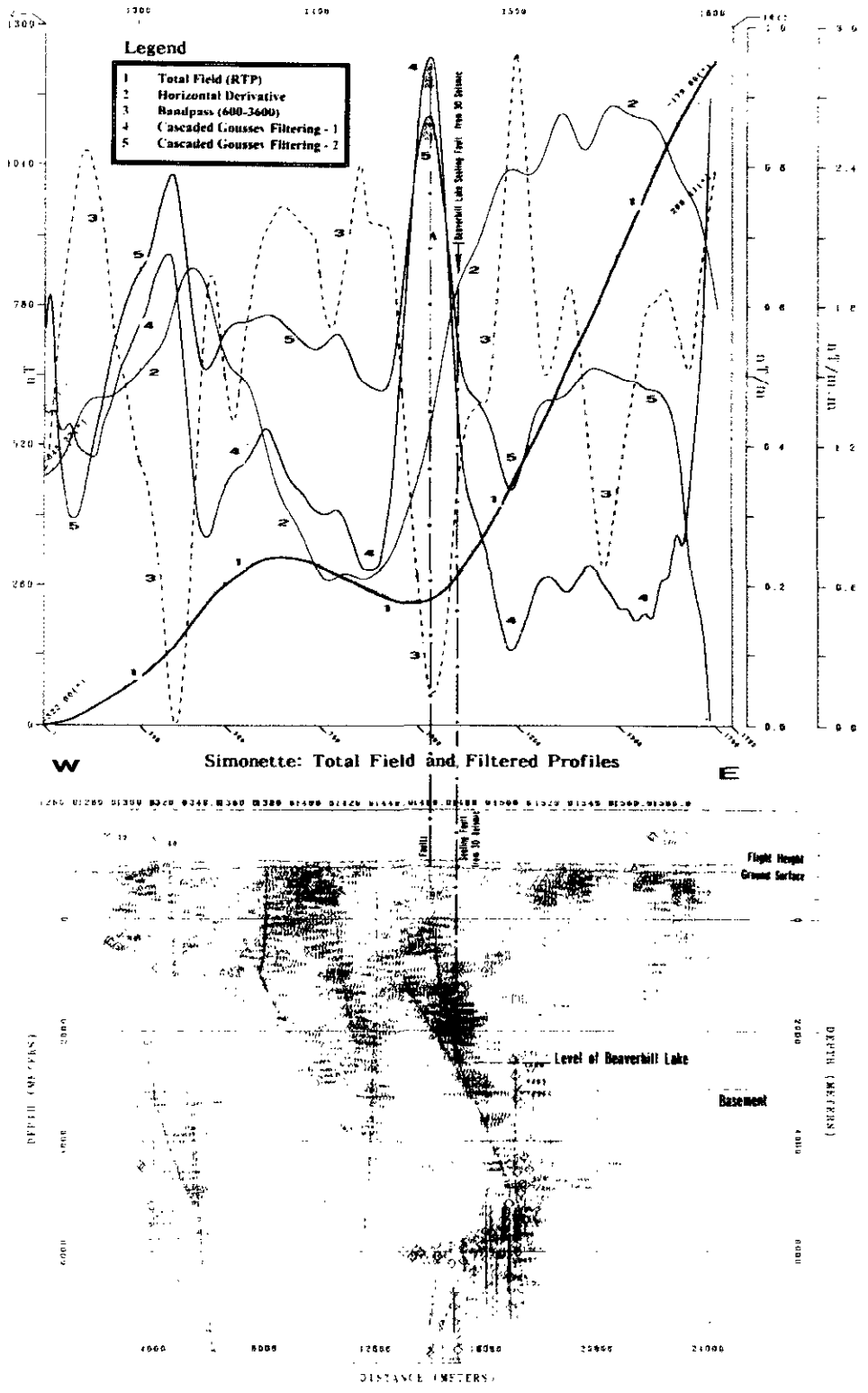


**Fig. 7.** Detailed interpretation of an east-west profile from the Simonette HRAM survey, crossing almost orthogonally to the Beaverhill Lake sealing fault. The upper portion shows the total magnetic field profile and its derivatives and two versions of the Cascaded Goussev Filter of the total field. The lower portion shows an interpretation of the Magprobe™ depth section along the profile. Red points are Werner deconvolution depth solutions. Green points are 2D Euler depth solutions. The seismically imaged sealing fault is indicated. The offset between the magnetic expression of the fault and the seismic position of the fault is discussed in the text.

## ACKNOWLEDGMENTS

We acknowledge L. Ollenberger of Chevron Canada Resources Ltd. for providing the 3D seismic structural map of the Simonette Beaverhill Lake pool. We also thank GEDCO staff for assistance in the preparation of this manuscript and, in particular, Mel Best for his detailed editorial comments.

## REFERENCES

Davies, G.R., 1997, Hydrothermal Dolomite (HDT) Reservoir Facies: Short Course Notes, CSPG-SEPM Joint Convention.

Ebner, E., Peirce, J.W., and Marchand, N., 1995, Interpretation of Aeromagnetic Data: CSEG Recorder, **20**, 8-11.

Jain, S., 1976, An automatic method of direct interpretation of magnetic profiles: Geophysics, **41**, 531-541.

_____, 1986, Structural mapping of the Precambrian surface using aeromagnetic data in the Peace River Area (abstract): CSEG Annual Meeting.

Jacobsen, B.H., 1987, A case for upward continuation as a standard separation filter for potential field maps: Geophysics, **52**, 1138-1148.

Ku, C.C., and Sharp, J.A., 1983, Werner deconvolution for automated magnetic interpretation and its refinement using Marquardt's inverse modeling: Geophysics, **48**, 754-774.

Ollenberger, L.S., 1996, Simonette Beaverhill Lake oil pool: discovery history, reservoir characterization and depletion strategy: CSPG Conference, Program and Abstracts.

Peirce, J.W., Ebner, E., and Marchand, N., 1998a, High-resolution aeromagnetic interpretation over Sierra and Yoyo Reefs, northeastern British Columbia, *in* Gibson, R.I., and Millegan, P.S., Eds., Geologic applications of gravity and magnetics: case histories: SEG Geophysical Reference Series No. 8, AAPG Studies in Geology, No. 43: Soc. Expl. Geophys. and Am. Assoc. Petr. Geol., 93-101.

_____, Goussev, S.A., Charters, R.A., Abercrombie, H.J., and DePaoli, G.R., 1998b, Intra-sedimentary magnetization by vertical fluid flow and exotic geochemistry: The Leading Edge, 17, 89-92.

Spector, A., and Grant, F.S., 1970, Statistical models for interpreting aeromagnetic data: Geophysics, **35**, 293-302.

Thompson, D.T., 1982, EULDPH – a new technique for making computer-assisted depth estimates from magnetic data: Geophysics, **47**, 31-37.

Werner, S., 1953, Interpretation of magnetic anomalies as sheet-like bodies: Sver. Geol. Undersok, ser. C., Arsbok **43**, N:06.